Comparison between lead free $BaTio_3$/PDMS and doped - PZT/PDMS composite on ferroelectric characteristics

L. Amarande[a], V. Stancu[a,*], M. Botea[a], V. Toma[a], R. Ciobanu[b], L. Pintilie[a]
[a]*National Institute of Materials Physics, Atomistilor 405A, 077125 Magurele, Ilfov Romania*
[b]*All Green SRL, Str. G. Cosbuc nr. 8, cod 700470, Iasi, Romania*

Composites of $BaTiO_3$ (BT) and doped-PZT (d-PZT) micro-particles randomly dispersed in a PDMS matrix were prepared by a molding process. The morpho-structural characterization, performed by SEM and XRD, showed ceramic micro-grains of cubic BT and orthorhombic d-PZT, randomly dispersed in the PDMS matrix. Polarization (*P)* as a function of the applied field (*E)* was measured for composite samples, as well as for polymer samples. Hysteresis loops typical for a dielectric material were obtained, but also atypical ones, especially for higher fraction of polymer in composite, lower fields and shorter measuring periods, as a result of the dielectric relaxation in polymer and the presence of interfacial polarization charges at the contact between polymer and ferroelectric. All these composites show very low polarizations (less than 0.2 μC/cm^2 and 0.05 μC/cm^2 the maximum and remnant polarization, respectively), caused by the very low dielectric constant of the polymer (less than 10), which drastically reduces, up to 100 times, the electric field effectively applied to the ferroelectric. Weak pyroelectric response was recorded on BT/PDMS, but a typical behavior of a pyroelectric detector was observed. A figure of merit of the material which exceeds 10^{-4} m^2/C was estimated.

(Received March 4, 2021, Accepted July 1, 2021)

Keywords: PDMS, Ferroelectric characteristics, Pyroelectric properties

1. Introduction

Composites of ferroelectric nano- or micro- particles, randomly dispersed in a polymer matrix are promising materials for sensors and energy harvesting applications, due to their cost effective, easy fabrication process, mechanical properties favorable to a variety of shapes, flexibility (flexible polymers), high electric energy densities and low dielectric loss [1-3]. By adjusting the ratio of the ferroelectric and polymer components, one can tailor the electrical and mechanical properties of the composite [4]. The main drawbacks of these particulate "0-3" composites consist in their weak ferroelectric and piezoelectric properties, as a result of the reduced connectivity between the ferroelectric particles, the high compliance of the polymer and the large mismatch of the dielectric constants of the two components, which requires considerably high poling fields (10 - 15 kV/mm) [5, 6].

These disadvantages can be partially overcome by structuring the composite through dielectrophoretic approach [7]. It consists in applying an a.c. field on the composite before curing the polymer, which aligns the ferroelectric particles in chains along the field, thus remaining fixed after curing the matrix. The resulting anisotropic composite will be more like a 1-3 composite, with stronger interactions between the structured particles, compared to randomly dispersed particles, resulting in increased piezoelectric and ferroelectric properties.

Polydimethylsiloxane (PDMS), is a suitable polymer for composite materials, which has been attracting a large interest in the field of electromechanical actuators, force sensors, piezoelectric generators and other stretchable electronics [8, 9], due to its high flexibility and dielectric breakdown field (100 MV/m).

* Corresponding author: stancu@infim.ro

In this work we studied the ferroelectric, dielectric and pyroelectric properties of the composites with barium titanate (BT) and doped lead titanate zirconate (d-PZT) randomly dispersed particles in a PDMS matrix.

2. Experimental section

Lead zirconate titanate ceramic doped with bismuth, iron and niobium $Pb_{0.98}Bi_{0.02}Zr_{0.5}Fe_{0.1}Nb_{0.09}Ti_{0.31}O_3$ (d-PZT) and barium titanate $BaTiO_3$, were prepared by the solid state synthesis method [10]. All the raw materials were purchased from Merck or Fluka with a purity greater then 99%. Ethanol 99,6% (Chimopar) was used as solvent. The raw materials were mixed in a RETSCH planetary ball mill at 300 rpm, for 2 hours for a good homogenization. The resulting powders were dried at 150°C and calcined at 900°C (d-PZT) and 1100°C (BT), respectively, for 2 hours. The PDMS (Sylgard 184, Dow Corning, U.S.A.) base and the curing agent with a mass ratio of 10:1 were mixed; then, the d-PZT as well as the BT powders (particle size between 2 and 10 μm) were immediately added into the uncured PDMS matrix. After being uniformly mixed, the uncured composite was put into a mold, in an oven, at 100 °C for 60 min. We obtained discs of 10 mm diameter and 1 mm thickness (Fig. 1).

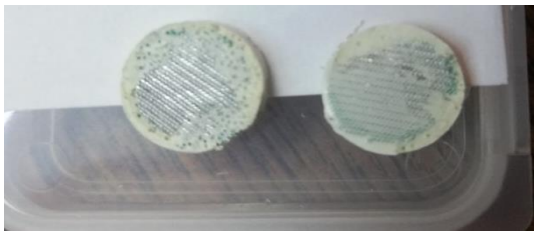

Fig. 1. Discs of BT/PDMS and d-PZT/PDMS composites with Al electrodes.

Two Al mesh electrodes (Good Fellow) were attached to the composite samples, before the polymer curing, for electric measurements. The morphology of the composite materials was studied with a Gemini 500 scanning electron microscope (SEM) (Carl Zeiss AG Germany). The crystal structure was analyzed by X-ray Diffraction (XRD) using a Bruker D8 Advance equipment (BRUKER-AXS GmbH, Germany).The parallel capacitance and the dissipation factor were measured at 1 kHz, with an AGILENT 4294 A Impedance Analyzer (Agilent Technologies, Santa Clara, CA), for dielectric characterization. The dielectric constant was calculated with the measured capacitance and the geometry of the samples. Polarization *P* as a function of the electric field *E* was measured with a Premier II ferroelectric test system (Radiant Technologies, Albuquerque NM, USA).

Pyroelectricity tests were performed in voltage mode, using a laser diode from Thorlabs with 808 nm wavelength (M9_808_0150) as an IR source. The laser beam was electronically modulated by a signal generator (Tektronix AFG 3052C), and the pyroelectric signal was recorded using a lock-in amplifier (SR 830 DSP - Stanford Research).

3. Results and discussion

The morphology of BT powders and d-PZT/PDMS disc samples was evidenced by SEM images shown in Fig.2 (a) and (b). They display a good packaging structure, with a homogeneous distribution of the ferroelectric grains in the PDMS matrix with very small pores.

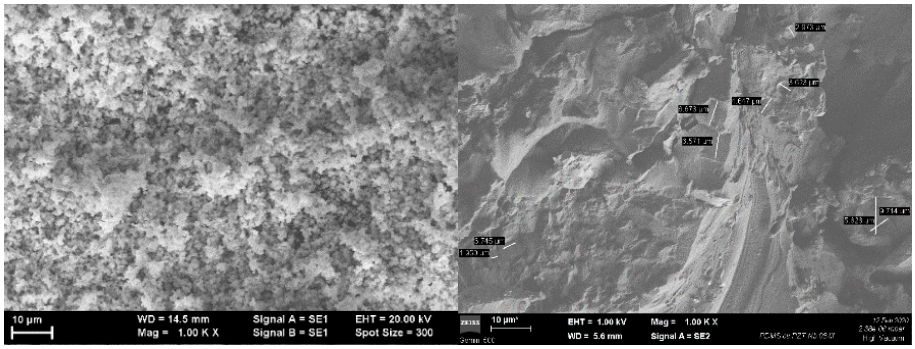

Fig. 2. SEM micrographs on BT powder and d –PZT/PDMS composite.

The XRD diffractograms of the composite discs, presented in Fig. 2, show the sharp and intense peaks corresponding to a cubic phase for BT and a single orthorhombic phase for d-PZT, indexed according to ASTM pattern 31-174 and ASTM 35-0739, respectively.

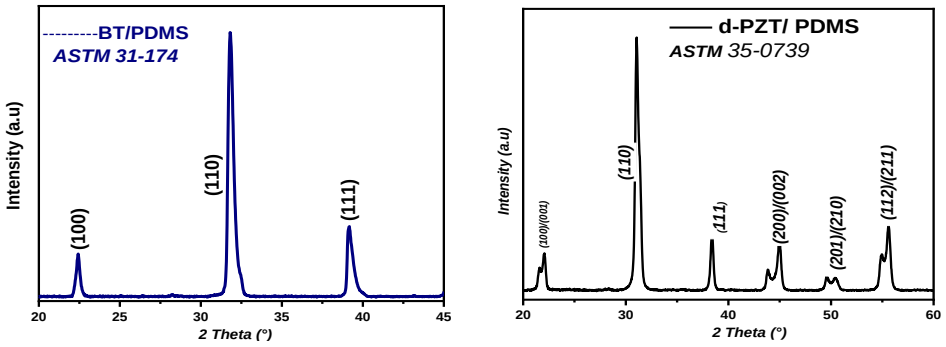

Fig. 3. XRD patterns of BT/PDMS and d- PZT/PDMS composites.

The poling procedure consisted in applying a high electric field, of about 10 kV/mm, on the polymerized composite samples, heated at 120°C, the temperature of the phase transition between the ferroelectric and paraelectric phase in BT, in order to align the dipols of the ferroelectric tetragonale phase, by the field, during the onset of this phase. The field was maintained during the cooling of the sample to the room temperature. However, only a small fraction of the applied field is effectively acting on the feroelectric particles in the composite, but at this phase transition, it is enough to ensure the polarization switching and allignement along the field. This could be an efficient approach for poling the composites, with low temperature phase transition ferroelectrics, such as BT and barium strontium titanate (BST). Yet, the proper poling conditions for a particular composite, should be found empirically. The d-PZT/PDMS composites were poled at the same temperature, only for increasing the mobility of the domains, their transition temperature being much higher.

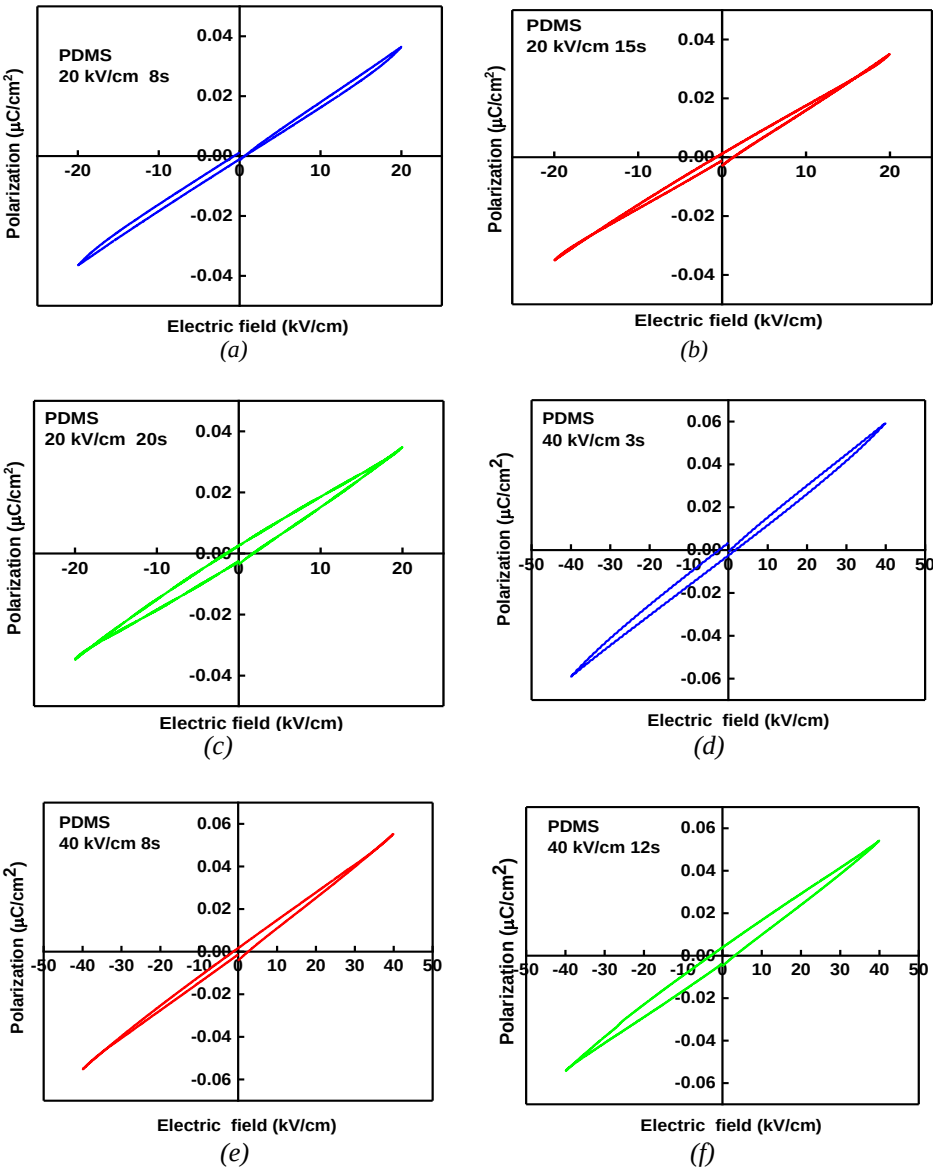

Fig. 4. P-E loops of PDMS samples, for maximum fields of 20 and 40 kV/cm and 3-20s periods.

Polarization (*P*) as a function of the bipolar triangular electric field (*E*), with maxima between 20 kV/cm and 90 kV/cm, was measured to evidence the ferroelectric properties of the composites. Hysteresis loops typical for a dielectric material were obtained, but also atypical ones, depending on the ratio of the ferroelectric-polimer, the amplitude and duration of the electric field, as will be further discussed. Therefore, we thoroughly studied the dependence *P-E* of the polymer samples, without ferroelectric, illustrated in Fig. 4 (a-f), for two amplitudes of the field (i.e. 20 and 40 kV/cm) and different durations, from 3s to 20s.

It is worthy noting the atypical aspect of the loops in Fig. 4 (a) and (d), with lower polarizations at the decreasing field, compared to those measured at the increasing field, for both polarities of the field, opposite to the case of normal dielectrics. The loops turn to a normal, wider shape with increasing the measurement time from 15s to 20s, for 20 kV/cm maximum field, as can be seen in Figs. 4(b) and (c), or from 8s to 12s, for 40 kV/cm field, as shown in Figs. 4(e) and (f) .

The pairs of loops in Fig. 4(a) and (d), (b) and (e) and (c) and (f), respectively are similar, even they correspond to different fields and durations, this suggesting an equivalence between the lower fields applied for longer time and the higher fields with shorter periods. This polymer behaviour influences the composite as well, especially at higher polymer ratios and lower fields

with shorter measuring periods. It can be correlated with dielectric relaxation in polymer and the presence of interfacial polarization charges at the contact between polymer and ferroelectric. The mechanism of polymer polarization needs to be further investigated, in order to explain this atypical behaviour. The *P-E* loops of BT/PDMS and d-PZT/PDMS composites, for maximum field of 70 kV/cm and 8s period, are represented in Fig. 5 (a) and (b) respectively.

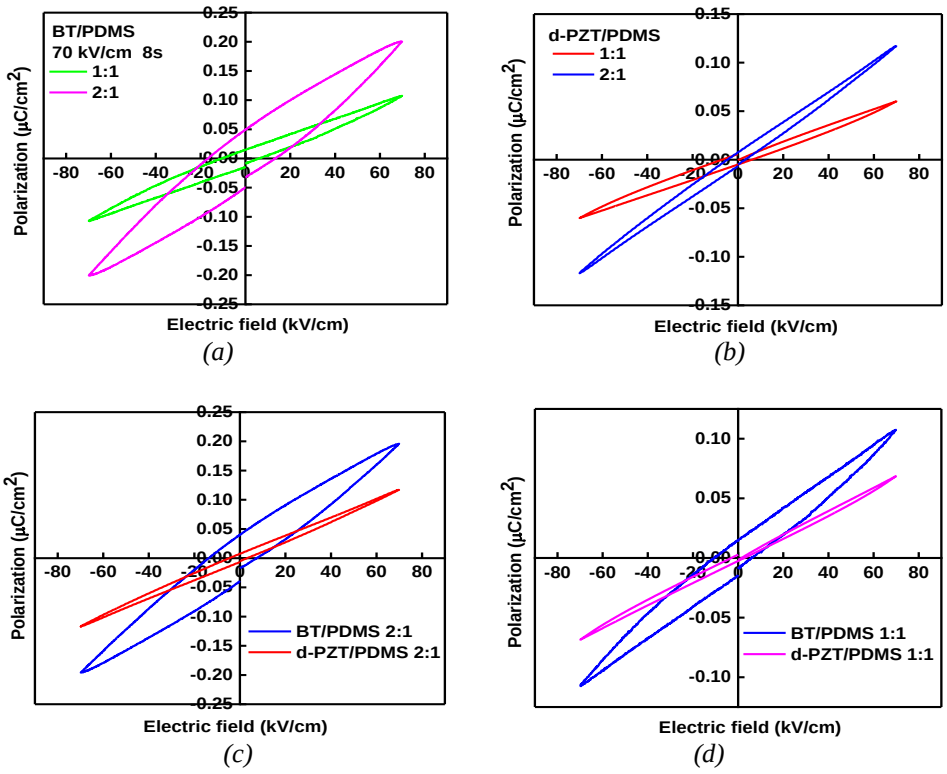

Fig. 5. P-E loops of BT/PDMS and d-PZT/PDMS composites.

The BT/PDMS loops have a normal shape, the one corresponding to higher amount of BT, being notably wider, with maximum and remanent polarization twice higher than for BT/PDMS 1:1.

The hysteresis loops of d-PZT based composites are very slim, with higher polarizations for higher amount of d-PZT. The d-PZT/PDMS 1:1 composite has an atypical loop, similar to those of Figs. 4 (a) and (d), as a result of the higher ratio of PDMS. The *P-E* loops of both type of composites are represented in Figs.5 (c) and (d) for each ratio of ferroelectric-polymer. The loops of d-PZT/PDMS are very slim, with lower maximum and remnat polarizations, compared to those of BT/PDMS. This can be explained by the difference between the molar mass of d-PZT (303 u.a.) and BT (233 u.a.), which results in a different number of mols (invers proportional to the molar mass), for the same weight ratio of ferroelectric-polimer.

The very low polarizations of these four composites (less than 0.2 μC/cm^2 and 0.05 μC/cm^2 the maximum and remnant polarization, respectively) are caused by the very low dielectric constant of the polymer (less than 10), which drastically reduces, up to 100 times, the electric field effectively applied to the ferroelectric, with a very high dielectric constant, higher than 1000.

The dielectric constant of a composite of randomly dispersed ellipsoidal particles in an isotropic matrix is given according to Yamada's model [11] by the following relationship:

$$\epsilon = \epsilon_1\left(1 + \frac{n\varphi(\varepsilon_2-\varepsilon_1)}{n\varepsilon_1+(\varepsilon_2-\varepsilon_1)(1-\varphi)}\right) \quad (1)$$

where ε is the composite permitivity, ε_1 and ε_2 are the permitivities of the matrix and of the particles, respectively, φ is the volume fraction of the particles in the composite and n is the inverse of the depolarization factor for an ellipsoidal particle, in the direction of the applied field. The electric field E_2 effectively applied to a ferroelectric particle in a polymer matrix, can be estimated, considering the particle and matrix as two series capacitors, by the following relation [7]:

$$\frac{E_2}{E} = \frac{(1+R)\varepsilon_1}{\varepsilon_2 + R\varepsilon_1} \tag{2}$$

where E is the field applied on the composite and R is the ratio between the particle size and interparticle distance.

In order to evidence the effect of poling on these composites, hysteresis loops were measured after poling. The first bipolar cycle registered after poling, begining with the poling polarity, is notably asymetrical, as can be seen in Fig. 6(a), (c) and (e), for BT/PDMS 1:1, 2:1 and d-PZT/PDMS 2:1, respectively.

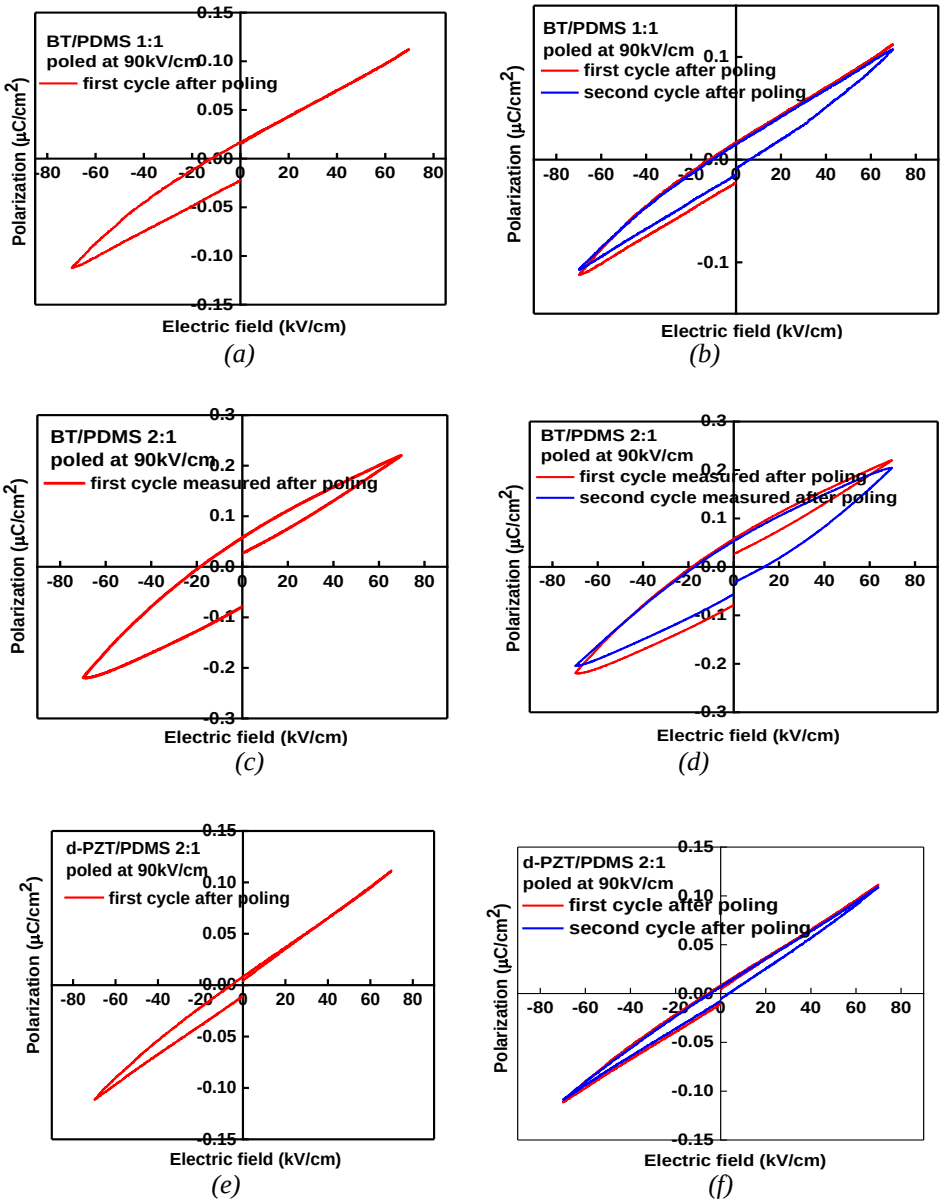

Fig. 6. The P-E loops registred at the first and second measurement cycles after poling, for: (a) and (b) BT/PDMS 1:1, (c) and (d) BT/PDMS 2:1,(e) and (f) d-PZT/PDMS 2:1.

For the positive polarity of the applied field, the same with that of the poling field, the loop is very slim, reduced to almost a line for BT/PDMS 1:1 and d-PZT/PDMS 2:1, since it represents only the reversible component of the polarization. After the second bipolar cycle, the loops become symetrical, since the remnant component of the polarization, resulting after poling, is also reversed. They are open, as a result of the dielectric loss.

The macroscopic piezoelectric response, expected after poling, could not be evidenced by impedance measurements, performed in a wide frequency range (40 kHz- 4 MHz), due to the very low remnant polarization. Neither clear differences between the capacitance and dielectric loss (see Table 1), measured at 1 kHz, before and after poling, were shown.

Table 1. The dielectric constant and loss of BT/PDMS and d-PZT/PDMS composites.

	BT/PDMS 1:1	**BT/PDMS 2:1**	**d-PZT/PDMS 1:1**	**d-PZT/PDMS 2:1**
Dielectric constant	10	18	6	12
Dielectric loss (10^{-3})	25	16	35	20

The degree of poling the composites could be enhanced by increasing the electrical conductivity, since the field acting on the ferroelectric particles depends on the dielectric constants of both phases, but also on the ratio of their conductivities [5], especially when the poling time is larger than the dielectric relaxation time [12]. The electrical conductivity of the composite is determined by the ratio of the conductive phase, which has to be optimized in order to prevent the whole composite becoming a conductor. There are experimental results reporting on the increasing degree of poling and of piezoelectric response, for an amount of 3.2 wt % carbon addition in BT/PDMS composites [13]. Enhanced dielectric performance of PDMS-based three-phase percolative nanocomposite films incorporating a high dielectric constant ceramic and conductive multi-walled carbon nanotubes was reported [14]. The hysteresis loops of BT/PDMS 1 :1 composites with and without carbon are represented in Fig. 7.

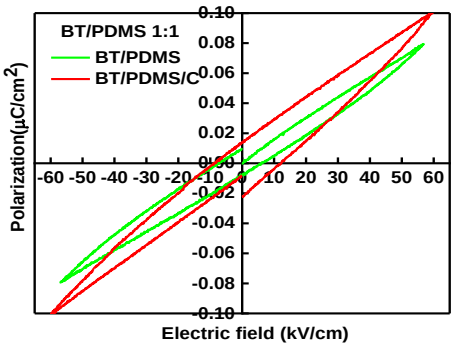

Fig. 7. P-E loops of BT/PDMS 1:1 with and without C addition.

The effect of 1 wt % carbon addition manifested in a slight increase of the maximum and remnant polarizations and the widen of the loops (due to the increased conductivity and dielectric loss). Similar results were obtained for d-PZT/PDMS composites.

The frequency dependence of the pyroelectric signal could only be recorded for BT/PDMS. The value of the pyroelectric signal was not very high, which was to be expected given the low polarization and capacitance values (< 0.2 μC/cm^2; 3 pF). However, a typical pyroelectric detector behavior was highlighted, have almost the same pyroelectric response at low frequencies and decreasing linearly at higher values.

$$S(\omega) = \frac{\eta p A P_{inc}}{\omega C_T C_e} \tag{3}$$

At high frequencies, S ≈ 1/ ω and the equation will replace to:

$$\frac{S(\omega)}{\frac{1}{\omega}} = \frac{p}{\varepsilon_0 \varepsilon_r \rho c} \cdot \frac{\eta P_{inc}}{A} = M \cdot \frac{\eta P_{inc}}{A} \tag{4}$$

The area of the electrodes is A= 80 mm^2, the emissivity η is ~ 0.05 for Al [15] and the incident power of the IR radiation is 30 mW. First factor represents the figure of merit of the material (M = p/$\varepsilon_0\varepsilon_r\rho c$) and it can be estimated from the slope of the representation S = f(1/ω) [16], Fig. 8. Also the physical quantities that appear in the ratio that defines the merit figure are: p the pyroelectric coefficient, c the specific heat of the material, ρ the density of the material, ε_r the dielectric constant of the material and ε_0 is the vacuum permittivity. For our case the value of the estimated figure of merit is 5.9·10^{-4} m^2/C.

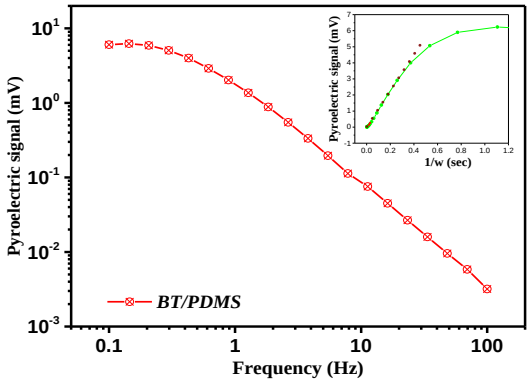

Fig. 8. Frequency dependence of the pyroelectric signal for BT/PDMS. Inset- S(ω) = f(1/ω).

4. Conclusions

BT/PDMS and d-PZT/PDMS particulate composites were prepared by a molding process allowing the control of the sample size and geometry. The morpho-structural characterization, performed by SEM and XRD, showed ceramic micro-grains of cubic BT and orthorhombic doped PZT, randomly dispersed in the PDMS matrix. The dependence of the polarization *P* as a function of the applied field *E* was investigated for composite samples, as well as for polymer samples. Hysteresis loops typical for a dielectric material were obtained, but also atypical ones, especially for higher fraction of polymer in composite, lower fields and shorter measuring periods. This is the result of the polymer behaviour, ascribed to the dielectric relaxation in polymer and the presence of interfacial polarization charges at the contact between polymer and ferroelectric.

The *P-E* loops of d-PZT/PDMS are very slim, with considerably lower maximum and remnat polarizations, compared to those of BT/PDMS. This can be explained by the higher poling level of BT/PDMS and by the difference between the molar mass of the two ferroelectric materials, which results in a lower numbers of d-PZT mols, for the same weight ratio of ferroelectric-polimer. All these composites show very low polarizations (less than 0.2 μC/cm^2 and 0.05 μC/cm^2 the maximum and remnant polarization, respectively), caused by the very low dielectric constant of the polymer (less than 10), which drastically reduces, up to 100 times, the electric field effectively applied to the ferroelectric, with a very high dielectric constant, higher than 1000.

The effect of poling was evidenced on these composites, by mesuring the first *P-E* bipolar cycle after poling,(begining with the poling polarity), which was notably asymetrical (very slim, reduced to almost a line for the poling polarity, as it represents only the reversible component of

the polarization). The effect of 1 wt % carbon addition to the composite samples manifested in a slight increase of the maximum and remnant polarizations and the widen of the hysteresis loops (due to the increased conductivity and dielectric loss).

The macroscopic piezoelectric response, expected after poling, could not be evidenced by impedance measurements, in the range of 40 kHz- 4 MHz, due to the very low remnant polarization. Neither clear differences between the capacitance and dielectric loss, measured at 1 kHz, before and after poling, were shown. All composites showed low dielectric constants (< 20). The material presented ferroelectric and pyroelectric properties. Weak pyroelectric response was recorded on BT/PDMS, but a typical behavior of a pyroelectric detector was observed. A figure of merit of the material which exceed 10^{-4} m^2/C was estimated.

Acknowledgements

The authors acknowledge funding through POC-G project MAT2IT (contract 54/2016), and the Core Program Core Program 2019-2022 (contract 21N/2019).

References

[1] J. Roedel, K. G. Webber, R. Dittmer, W. Jo, M. Kimura, D. Damjanovic, J. Eur. Ceram Soc. **35**(6), 1659 (2015).
[2] P. H. Hu, Y. Shen, Y. H. Guan, X. H. Zhang, Y. H. Lin, Q. M. Zhang, C. W. Nan, Adv. Funct. Mater. **24**(21), 3172 (2014).
[3] X. Zhang, Y. Shen, B. Xu, Q. H. Zhang, L. Gu, J. Y. Jiang, J. Ma, Y. H Lin, C. W. Nan, Adv. Mater. **28**(10), 2055 (2016).
[4] R. E. Newnham, D. P. Skinner, L. E. Cross, Mater Res. **13**, 525 (1978).
[5] G. Sa-Gong, A. Safari, S. J. Jang, E. Newnham, Ferroel. Lett. **5**(5), 131 (1986).
[6] D. B. Deutz, N. T. Mascarenhas, S. van der Zwaag, W. A. Groen, Ferroelectrics **515**, 68 (2017).
[7] D. A. van den Ende, B. F. Bory, W. A. Groen, S. van der Zwaag, J. Appl. Phys. **107**, 024107 (2010).
[8] H. Jang, H. Yoon, Y. Ko, J. Choi, S. S. Lee, I. Jeon, J. H. Kim, H. Kim, Nanoscale **8**(10), 5667 (2016).
[9] M. D. Dickey, P. Gaiser, J. Binz, B. Gompf, A. Berrier, M. Dressel, Nanoscale **7**(10), 4566 (2015).
[10] V. Stancu, L. Amarande, M. Botea et al., Processing and Application of Ceramics **13**(3), 269 (2019).
[11] T. Yamada, T. Ueda, T. Kitayama, J. Appl. Phys. **53**, 4328 (1982).
[12] C. K. Wong, F. G. Shin, J. Appl. Phy. **97**, 034111 (2005).
[13] C. Luo, S. Hu, M. Xia, P. Li, J. Hu, G. Li, H. Jiang, W. Zhang, Energy Technol. **6**(5), 922 (2017).
[14] G. Liu, Y. Chen, M. Gong, X. Liu, Z-K. Cui, Q. Pei, J. Gu, C. Huanga, Q. Zhuang, J. Mater. Chem. C **6**, 10829 (2018)
[15] https://www.scribd.com/doc/83065506/tabel-emisivitati
[16] V. Stancu, L. Amarande, M. Botea, M. Cioangher, A. G. Tomulescu, A. Iuga, L. Pintilie, Digest Journal of Nanomaterials and Biostructures **14**(1), 225 (2019).